Optics Letters

Power-scalable thin-disk Ti:sapphire laser amplifier

JIANWANG JIANG,[1] XU ZHANG,[1] ZHAOHUA WANG,[1] HAO TENG,[1] SHAOBO FANG,[1,3,4] JIANGFENG ZHU,[2] AND ZHIYI WEI[1,3,4,*]

[1]*Beijing National Laboratory for Condensed Matter Physics, Institute of Physics, Chinese Academy of Sciences, Beijing 100190, China*
[2]*School of Optoelectronic Engineering, Xidian University, Xi'an 710071, China*
[3]*University of Chinese Academy of Science, Beijing 100049, China*
[4]*Songshan Lake Material Laboratory, Dongguan 523808, China*
*Corresponding author: zywei@iphy.ac.cn*

We experimentally demonstrate a 38-fs chirped-pulse amplified (CPA) Ti:sapphire laser system based on the power-scalable thin-disk scheme with an average output power of 1.45 W at a repetition rate of 1 kHz, corresponding to peak power of 38 GW. The beam profile close to the diffraction limit with a measured M^2 value of approximately 1.1 is obtained. It demonstrates the potential for an ultra-intense laser with high beam quality compared with the conventional bulk gain amplifier. To the best of our knowledge, this is the first reported Ti:sapphire regenerative amplifier based on the thin-disk approach reaching 1 kHz. © 2022 Optica Publishing Group

Since the concept of thin-disk lasers was first presented in 1994 [1], ultrafast thin-disk lasers have become a promising laser source for a vast number of applications in micromachining [2], high-harmonic generation (HHG) [3–5], high-field science [6], and generation of mid-infrared pulses [7]. Ultrafast thin-disk lasers have more advantages in terms of thermal management than conventional bulk lasers, resulting in higher repetition rate, higher average power, higher pulse energy, as well as better beam quality [8–10]. Yb-doped materials, especially Yb:YAG, have been the most significant gain media used for thin-disk laser amplifiers with regenerative or multi-pass configuration because of easy growth, sufficiently large emission bandwidth supporting the generation of femtosecond pulses, the availability of suitable high-power diode pump sources, small quantum defect, high doping concentration, and so on [11,12]. To date, the bulk Yb-doped multistage chirped-pulse amplified (CPA) laser amplifier has been developed with pulse energies of 67 mJ and pulse duration of 3 ps at 1.25 kHz employing complicated cryogenic cooling [13]. Meanwhile, pulse energies as high as 200 mJ [14] and average output power up to 1.9 kW [15] were reached from thin-disk Yb:YAG laser amplifiers. The above-mentioned thin-disk laser amplifiers have a pulse duration of a few picoseconds and operate at low repetition rates. Thanks to the introduction of chirped-pulse amplification [16] and the progress of thin-disk welding or bonding technologies with a heat sink [17], the performances of thin-disk laser amplifiers were dramatically promoted. A thin-disk regenerative laser amplifier with the pulse energy of 550 mJ at a repetition rate of 1 kHz was reported in 2021 [18]. A diode-pumped multistage Yb:YAG laser amplifier based on the CPA scheme was demonstrated with a pulse energy of up to 1.1 J and pulse duration of 4.5 ps at 1 kHz [19].

The remarkable success in Yb-doped thin-disk lasers has drawn attention to other excellent gain media such as Tm:LiYF$_4$, Nd:YVO$_4$, Tm:KLu(WO$_4$)$_2$ [20–22]. Moreover, the proven Ti:sapphire crystal has also gradually come into people's vision again. as it has the broadest optical absorption and gain bandwidth than any other laser gain material [23], supporting less than 5-fs pulse duration directly generated from a laser oscillator [24] and sub-13-fs pulse duration from a laser amplifier [25]. Moreover, the Ti:sapphire crystal has superior thermodynamic and mechanical properties suitable for the multi-pass thin-disk structure. In 2016, Chvykov *et al.* reported a high peak and average output power broadband Ti:sapphire thin-disk laser amplifier at a repetition rate of 10 Hz, which combined the extraction during a pumping amplification scheme and the thin-disk technology [26]. The highest optical efficiency of 11% was achieved under 48 pump laser passes. In 2019, a multi-passed Ti:sapphire laser amplifier based on the cross thin slab scheme was proposed [27], where laser pulses with multi-mJ pulse energy and kW average power level were generated. In the meantime, numerical simulations were presented [28,29], which analyzed the thermal distribution of the thin-disk Ti:sapphire crystal and predicted that an approximately 300-W average power could be reached in the near future with doubled-sided cooling arrangements [30]. Due to the quantum defect of higher than 33%, a large amount of heat accumulation is inevitable, which leads to thermal lensing and aberrations. This will affect the further improvement of the output parameters for a bulk Ti:sapphire laser amplifier. It is necessary to explore a new approach to further increase the output average power or pulse energy of Ti:sapphire laser amplifiers. Naturally, the power-scalable thin-disk scheme becomes a choice, which is expected to obtain ultrashort laser pulses with high beam quality at the high output power levels. However, we must consider that the sufficient pump wavelength of Ti:sapphire lasers is usually in the blue-green spectral region, which limits to the availability of the suitable high-power diode lasers. Therefore, designing a multi-pass pump structure with an all-solid-state pump laser is also a required work.
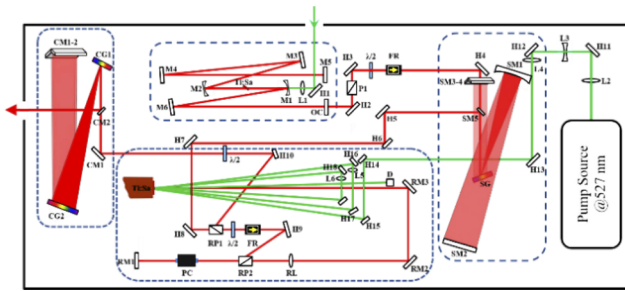
Fig. 1. Schematic diagram of the experimental setup. M1–M6, double-chirped mirror pairs; OC, output coupler; H1–H18, 45° highly reflective mirror; P1, RP1, RP2, Glen–Taylor polarizer; λ/2, half-wave plate; FR, Faraday rotator; SG, CG1, CG2, holographic grating; SM1, spherical mirror (ROC = 1219.2 mm); L1–L6, pump lens; Ti:Sa, thin-disk Ti:sapphire crystal. RL, thin lens (f = 1.2 m); PC, Pockels cell; RM1–RM3, highly reflective mirror inside the generative cavity; D, dump. The total length of the regenerative cavity is 1.5 m.

Fig. 2. Spectrum of the thin-disk Ti:sapphire laser amplifier within each stage. The green line represents the spectrum of the seed pulse, the red curve after the Martinez stretcher, the black line after the regenerative laser amplifier, and the blue line represents the phase after the compressor.

In this paper, we demonstrate the feasibility of a chirped-pulse regenerative laser amplifier based on the power-scalable thin-disk Ti:sapphire scheme. The laser system delivers an average output power of 1.45 W and 38-fs pulse duration, corresponding to a peak power of 38 GW at a repetition rate of 1 kHz. A pulse beam close to the diffraction limit with a measured M^2 value of 1.1 is obtained. We believe that the thin-disk Ti:sapphire amplifier is a potential way to replace the bulk Ti:sapphire laser amplifiers.

Figure 1 shows the schematic diagram of the whole experimental setup. An all-chirped-mirror Ti:sapphire laser oscillator operating at 83 MHz was built as the seed source of the CPA laser amplifier, which was capable of producing more than 350-mW average output power under the pump power of 3.2 W and a spectrum covering from 700 nm to 950 nm, as shown by the green curve shown in Fig. 2. It should be clear that the peak at 730 nm arises from the dispersion-matched phase wave instead of CW or the misalignment of the Ti:sapphire laser oscillator. The seed pulses were aligned through a Faraday isolator (including P1, λ/2, and FR) and sent into a self-built Martinez stretcher. Approximately 20-fs pulses were temporally stretched to approximately 300 ps before the seed pulses were injected into the regenerative laser amplifier. The spectrum after the Martinize stretcher is given as the red curve in Fig. 2. The narrowing spectrum originated from the coating bandwidth of the mirrors and the finite size of the diffraction grating used in the experiment. The stretched seed pulses were then injected into the thin-disk Ti:sapphire regenerative laser amplifier with the linear cavity length of 1.5 m. A regenerative laser amplifier has the advantages of better output beam quality, higher amplificated efficiency, and simple structure for alignment compared with a multi-pass laser amplifier. A 2-mm-thick Ti:sapphire disk was employed as the end mirror coated with antireflective coating on the front facet and a highly reflective coating on the other facet for both the pump and laser wavelengths at 700–900 nm, which was mounted on a W80Cu20 heat sink maintained at 14°C during the experiment. The thermal load can be effectively reduced by the circulating water. To tune the cavity mode, a thin lens (RL) with the focal length of 1.2 m was placed approximately 1 m away from the Ti:sapphire disk. The laser mode radius on the disk was calculated to be approximately 0.4 mm with the ABCD
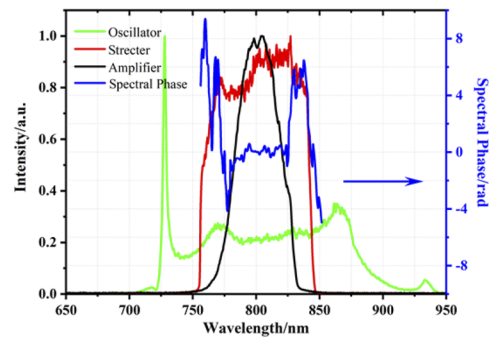
Matrix. The pump laser is a diode-pumped frequency-doubled solid-state laser delivering the highest average power of 20 W at 527 nm with a repetition rate of 1 kHz. To match up with the laser mode, a series of thin lenses (f_{L2} = 800 mm, f_{L3} = −200 mm, f_{L4}, f_{L6} = 300 mm, f_{L5} = 400 mm) were used to adjust the pump spot on the disk to approximately 1.2 mm in diameter, which can sufficiently avoid damage of the coating layer caused by the high peak power of Gauss beam. The 6-fold passage of the pump laser through the disk was adopted to obtain an absorption efficiency of more than 90%. More pump passages were limited due to the large fold angle increased pump loss.

Initially, an output coupler with a transmission of 10% at 700–900 nm was placed at the end mirror RM1 to realize the gain-switched operation. Then, the Ti:sapphire disk was rotated to achieve the highest absorption for the pump laser and the broadest output spectrum. Subsequently, a Pockels cell (PC) and a Glen–Taylor polarizer (RP) were successively inserted inside the regenerative cavity. Finally, the end mirror RM1 was taken to replace the output coupler. The stretched seed pulses were sent into the regenerative cavity through reflective mirrors H6 and H7. When the status of the regenerative cavity and the overlap of the pump laser, as well as the laser mode on the Ti:sapphire disk, were adjusted to be optimal, the laser pulses performed 45 round trips inside the regenerative cavity. We directly obtained the maximum average output power of 1.8 W with an incident pump power of 16 W at a repetition rate of 1 kHz. The amplified efficiency of approximately 11% was achieved. At the maximum output power of the regenerative cavity, we were able to determine the total group delay dispersion and third-order dispersion induced by the dispersive materials and optical path. The optimal settings of the grating compressor, including the grating separations and grating incidence angles, were designed to recompress the pulse duration to be as short as possible. The compressor consisted of two gold-coated holographic gratings with grooves of 1500 lines/mm. After the compressor, 1.45-W output power was obtained, corresponding to an efficiency of approximately 80%. The compressed pulse spectrum is given as the black curve in Fig. 2, which supports an approximately 28-fs Fourier transformation limited pulse. An actual pulse duration as short as 38 fs was directly measured by a commercial Wizzler after optimized compression, as shown in Fig. 3. The reason may be that the high-order dispersion of the laser material was not well compensated. We measured
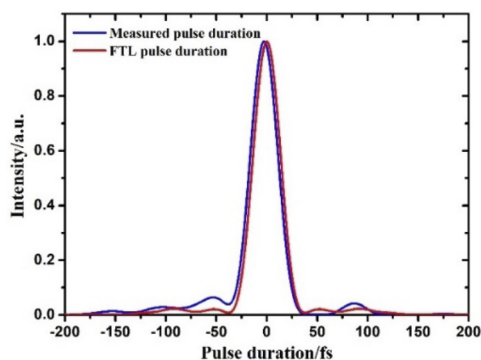
Fig. 3. Measured pulse duration after the compressor and the Fourier transform limited pulse duration.
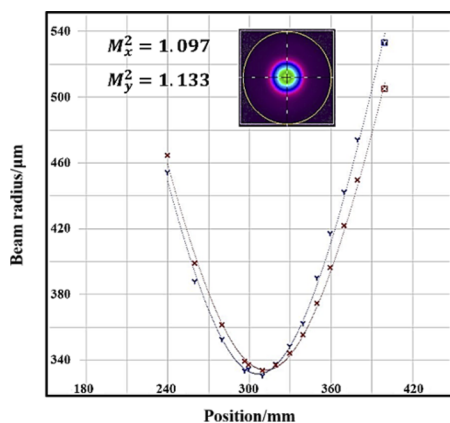

**Fig. 4.** Near-field beam profiles and M^2 factor after the compressed pulse.

the beam profile using a commercial beam analyzer. The near-field beam profile and M^2 factor of the compressed pulse after the compressor are shown in Fig. 4. The calculated M^2 factors are $M_x^2 = 1.097$ and $M_y^2 = 1.133$. The output spot indicates that the amplifier operates in the fundamental mode of the near-Gaussian beam.

Due to the lack of high-power laser diodes (LD) in the green-blue wavelength region, we employed an all-solid-state pump laser and highly reflective mirrors at 527 nm to build a multi-pass pump module in our experiments. The limited pump passage made it necessary to use a thicker gain crystal, which resulted in a high thermal load inside the Ti:sapphire crystal, as shown in Fig. 5(d). Moreover, A higher pump power was avoided to limit damage to the rear coating of the Ti:sapphire crystal, because the welding process of the Ti:sapphire crystal with a heat sink decreases the damage threshold of the rear coating of the crystal. The damage threshold of the rear highly reflective coating is estimated to be only 0.45 J/cm². It is believed that a higher output power can be obtained with a higher damage threshold of the coating layer. In addition, to obtain a high output beam quality and protective coating on Ti:sapphire crystal, the modes of the pump laser and gain laser are largely mismatched in the amplification process. This decreases the energy extraction efficiency.

To prove the potential of a thin-disk Ti:sapphire scheme, the thermal distribution inside a Ti:sapphire crystal with a different thickness was analyzed by finite element analysis, as shown in
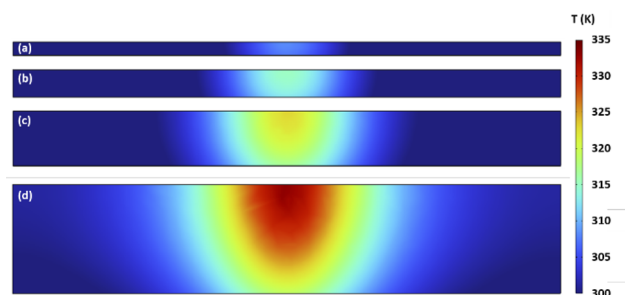

Fig. 5. Thermal distribution in the thin disk for different thick Ti:sapphire crystal: (a) 0.25 mm; (b) 0.5 mm; (c) 1 mm; (d) 2 mm. The pumping condition is 100-W pump power at a repetition rate of 1 kHz. The laser beam radius on the Ti:sapphire crystal is estimated to be 625 µm. The heat sink is W80Cu20.
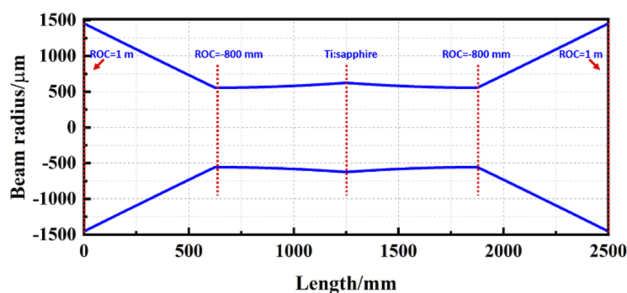
Fig. 6. Mode evolution of the improved regenerative cavity.

Fig. 5. The central temperature of the 2-mm-thick disk is up to 61°C and there is a larger thermal gradient along the axial direction under the pump energy of 100 mJ at 1 kHz, as well as the radius of 625 µm on the Ti:sapphire crystal. As the thickness of the gain crystal decreases, both the temperature at the center of the Ti:sapphire crystal and the axial thermal gradient are significantly reduced. The central temperature for a 0.25-mm-thick Ti:sapphire crystal is only 34°C and the axial thermal gradient is also smaller under the same pump conditions. At this time, according to the absorption coefficient of ~7.5 cm⁻¹, the pump passage of 16 passes must be reached to achieve an efficient absorption rate of up to 95%. Based on the pump conditions as described above, we have simulated a more suitable regenerative cavity, as described in Fig. 6. The regeneration cavity consists of two concave mirrors (ROC = 1 m), two convex mirrors (ROC = −0.8 m), and a thin-disk Ti:sapphire crystal as the active mirror. The thin-disk Ti:sapphire crystal is located in the center of the regeneration cavity. The amplificated laser pulses pass through the Ti:sapphire crystal four times per round trip to increase the energy extraction efficiency. In addition, a power scalability can be achieved by adjusting the distance of the two convex mirrors from the crystal. This improved regenerative cavity design not only increases the size of the pump on the thin-disk Ti:sapphire crystal, but also enables power scalability and increases the output power under the premise of ensuring the crystal coating. This new scheme will greatly increase the potential of thin-disk Ti:sapphire regenerative laser amplifiers and reduce the complexity of the system by removing the structures such as thermo electric cooler and the vacuum chamber.

We also analyzed the heat distribution inside the Ti:sapphire crystal with different heat sink materials under the same pump conditions. The simulated results are shown in Fig. 7. The
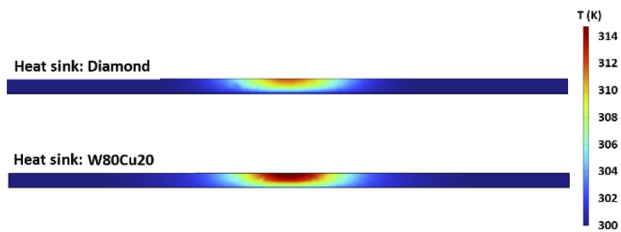
Fig. 7. Heat distribution of the different heat sink materials.

heat conductivity of the W80Cu20 metal and diamond are 210 W/m·K and 2000 W/m·K at room temperature, respectively. Although there is a huge difference in the thermal conductivity between the two materials, the thermal accumulation is not very obvious for a 250-μm-thick gain crystal. It is favorable to economically obtain a power-scaling thin-disk Ti:sapphire laser amplifier to replace the regenerative or multi-pass bulk Ti:sapphire laser amplifier.

In conclusion, a Ti:sapphire regenerative amplifier based on CPA technology and a power-scalable thin-disk scheme is demonstrated. It delivers an average output power of 1.45 W, 38-fs pulse duration, and peak power of 38 GW at a repetition rate of 1 kHz. An M^2 of approximately 1.1 is measured, which is close to the diffraction limit. Further, the thermal distribution varies with the thick of gain medium and different heat sink materials are analyzed to prove the potential of the thin-disk Ti:sapphire laser amplifier. We believe that better results will be obtained in the following experiment by means of using a thinner Ti:sapphire crystal, such as 0.25 mm, and an improved multi-pass pump module with more than 16 passes. This will pave the way to obtain high-power, sub-30-fs pulses, and a high beam quality close to the diffraction limit by a power-scaling thin-disk Ti:sapphire laser amplifier at a few kilohertz.

Disclosures. The authors declare no conflicts of interest.

Data availability. Data underlying the results presented in this paper are not publicly available at this time but may be obtained from the authors upon reasonable request.

REFERENCES

1. A. Giesen, H. Hügel, A. Voss, K. Wittig, U. Brauchand, and H. Opower, Appl. Phys. B **58**, 365 (1994).
2. R. Gattass and E. Mazur, Nat. Photonics **2**, 219 (2008).
3. J. Fischer, J. Drs, F. Labaye, N. Modsching, V. J. Wittwer, and T. Südmeyer, Opt. Express **29**, 5833 (2021).
4. F. Emaury, A. Diebold, C. J. Saraceno, and U. Keller, Optica **2**, 980 (2015).
5. F. Labaye, M. Gaponenko, V. J. Wittwer, A. Diebold, C. Paradis, N. Modsching, L. Merchron, F. Emaury, I. J. Graumann, C. R. Phillips, C. J. Saraceno, C. Kränkel, U. Keller, and T. Südmeyer, Opt. Lett. **42**, 5170 (2017).
6. T. Südmyer, S. V. Marchese, S. Hashimoto, C. R. E. Baer, G. Gingras, B. Witzel, and U. Keller, Nat. Photonics **2**, 599 (2008).
7. I. Pupeza, D. Sánchez, J. Zhang, N. Lilienfein, M. Seidel, N. Karpowicz, T. Paasch-Colberg, I. Znakovskaya, M. Pescher, W. Schweinberger, V. Pervak, E. Fill, O. Pronin, Z. Wei, F. Krausz, A. Apolonski, and J. Biegert, Nat. Photonics **9**, 721 (2015).
8. S. V. Marchese, T. Südmeyer, M. Golling, R. Grange, and U. Keller, Opt. Lett. **31**, 2728 (2006).
9. O. H. Heckl, C. Kränkel, C. R. E. Baer, C. J. Saraceno, T. Südmeyer, K. Petermann, G. Huber, and U. Keller, Opt. Express **18**, 19201 (2010).
10. J. Zhang, M. Pötzlberger, Q. Wang, J. Brons, M. Seidel, D. Bauer, D. Sutter, V. Pervak, A. Apolonski, K. F. Mak, V. Kalashnikov, Z. Wei, F. Krausz, and O. Pronin, Ultrafast Science **2022**, 1 (2022).
11. T. Südmeyer, C. Kränkel, C. R. E. Baer, O. H. Heckl, C. J. Saraceno, M. Golling, R. Peters, K. Petermann, G. Huber, and U. Keller, Appl. Phys. B **97**, 281 (2009).
12. T. Taira, W. M. Tulloch, and R. L. Byer, Appl. Opt. **36**, 1867 (1997).
13. F. X. Morrissey, T. Y. Fan, D. E. Miller, and D. Rand, Opt. Lett. **42**, 707 (2017).
14. T. Nubbemeyer, M. Kaumanns, M. Ueffing, M. Gorjan, A. Alismail, H. Fattahi, J. Brons, O. Pronin, H. G. Barros, Z. Major, T. Metzger, D. Sutter, and F. Krausz, Opt. Lett. **42**, 1381 (2017).
15. T. Dietz, M. Jenne, D. Bauer, M. Scharun, D. Sutter, and A. Killi, Opt. Express **28**, 11415 (2020).
16. D. Strickland and G. Mourou, Opt. Commun. **55**, 447 (1985).
17. A. Giesen and J. Speiser, IEEE J. Sel. Top. Quantum Electron. **13**, 598 (2007).
18. Y. Pfaff, M. Rampp, C. Herkommer, R. Jung, C. Y. Teisset, S. Klingebiel, and T. Metzger, in *Laser Congress 2021 (ASSL,LAC)*, (Optica Publishing Group, 2021), paper bo.
19. Y. Wang, H. Chi, C. Baumgarten, K. Dehne, A. R. Meadows, A. Davenport, G. Murray, B. A. Reagan, C. S. Menoni, and J. J. Rocca, Opt. Lett. **45**, 6615 (2020).
20. R. Soulard, M. Salhi, G. Brasse, P. Loiko, J.-L. Doualan, L. Guillemot, A. Braud, A. Tyazhev, A. Hideur, and P. Camy, Opt. Express **27**, 9287 (2019).
21. P. Millar, A. J. Kemp, and D. Burns, Opt. Lett. **34**, 782 (2009).
22. S. Vatnik, I. Vedin, M. Segura, X. Mateos, M. C. Pujol, J. J. Carvajal, M. Aguiló, F. Díaz, V. Petrov, and U. Griebner, Opt. Lett. **37**, 356 (2012).
23. P. F. Moulton, J. Opt. Soc. Am. B **3**, 125 (1986).
24. R. Ell, U. Morgner, F. X. Kärtner, J. G. Fujimoto, E. P. Ippen, V. Scheuer, G. Angelow, T. Tschudi, M. J. Lederer, A. Boiko, and B. Luther-Davies, Opt. Lett. **26**, 373 (2001).
25. M. Musheghyan, F. Lücking, Z. Cheng, H. Frei, and A. Assion, Opt. Lett. **44**, 1464 (2019).
26. V. Chvykov, H. Cao, R. Nagymihaly, M. P. Kalashnikov, N. Khodakovskiy, R. Glassock, L. Ehrentraut, M. Schnuerer, and K. Osvay, Opt. Lett. **41**, 3017 (2016).
27. H. Cao, R. S. Nagymihaly, and V. Chvykov, Laser Phys. **29**, 065802 (2019).
28. V. Chvykov, R. S. Nagymihaly, H. Cao, M. Kalashnikov, and K. Osvay, Opt. Express **24**, 3721 (2016).
29. N. Hodgson and A. Caprara, Appl. Opt. **55**, 5110 (2016).
30. R. S. Nagymihaly, H. Cao, D. Papp, G. Hajas, M. Kalashnikov, K. Osvay, and V. Chvykov, Opt. Express **25**, 6664 (2017).